Two-Dimensional Discrete Cavity Solitons: Switching and All-Optical Gates

K. M. Aghdami
M. Golshani
R. Kheradmand
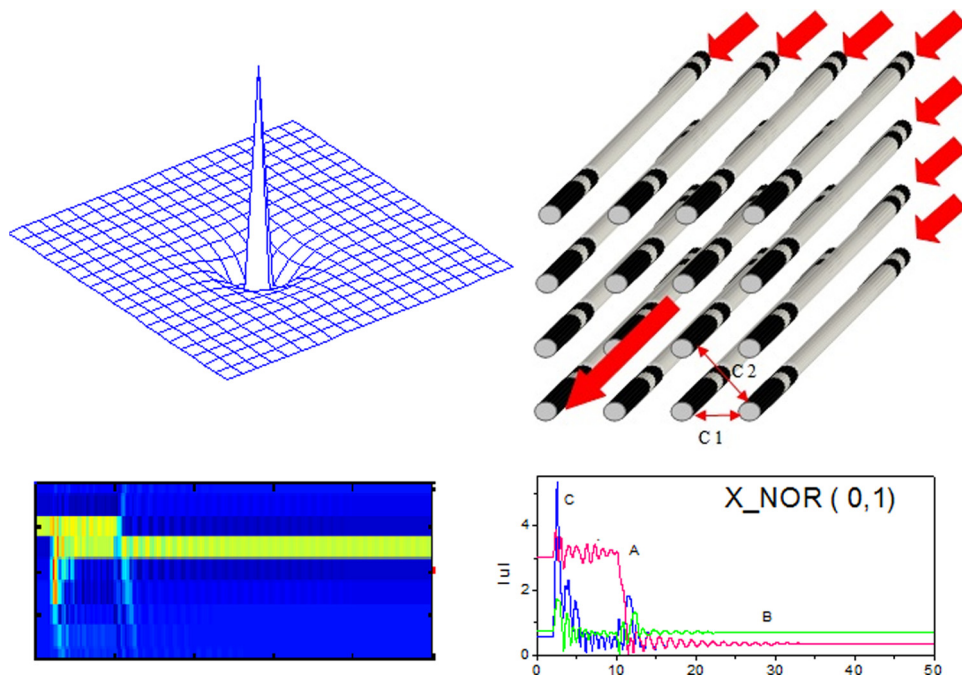
Two-Dimensional Discrete Cavity Solitons: Switching and All-Optical Gates

K. M. Aghdami,[1,2] **M. Golshani,**[1] **and R. Kheradmand**[1]

[1]Photonics Group, Research Institute for Applied Physics and Astronomy,
University of Tabriz, Tabriz, Iran
[2]Department of Physics, Payame Noor University, Tehran, Iran

Abstract: Light propagation in a 2-D array of coupled optical cavities with Kerr nonlinearity driven by a plane holding beam is numerically studied. Optical bistability together with its modulational instability (MI) are investigated, and 2-D discrete cavity solitons are simulated. These simulations revealed the switching on/off of the solitons along with the ability of a proper Gaussian beam (GB) to control their positions. Soliton–soliton and soliton–GB interactions are considered, and finally, all-optical NOR, XNOR, and NAND gates are proposed as realized by this device.

Index Terms: Nonlinear, Kerr effect, soliton, ultra fast devices.

1. Introduction

Recently, experimental and theoretical studies on light localization in discrete optical systems have taken much interests; a typical example of such cases is an array of coupled waveguide. The peculiarities of discrete diffraction allow for the formation of new types of spatially localized solutions, so-called discrete solitons [1]–[3]. An array of coupled-waveguide resonators is constructed through addition of mirrors to the input and output facets of the waveguide array, which is excited by an external driving field [4]. Multiple reflections of light on the mirrors increase in light interaction with the nonlinear material inside the cavity causes to form discrete cavity solitons (DCSs) at substantially less powers in comparison with conventional spatial solitons in single pass configuration. Simultaneous excitation of bright and dark DCSs in the same array of coupled waveguides in one of unique features of these systems. The existence of DCSs in system with internal feedback, which is a result of the interplay among nonlinearity, diffraction as well as gain, losses has been predicted for quadratic [5], saturable [6], [7], and Kerr media in one-dimension [8]–[10]. The investigation of the coupling between highly equivalent waveguides and nonlinear localization along with strong boundary effects is the key to understand nonlinear discrete propagation in 2-D lattices for future applications [11]. The first observation of a 2-D discrete soliton was achieved in optically induced waveguide arrays in photorefractive materials [12]. The possibility of realizing useful functional operations with discrete solitons such as blocking, routing, and gating can be provided by 2-D networks of nonlinear waveguides [13], [14]. There is a great interest in all-optical switching devices based on the optical Kerr effect in a nonlinear waveguide for high-bit rate optical communication and ultrafast information processing systems [15], [9], [10]. In the past, several all-optical switching devices have been proposed by using a nonlinear interferometer [16], [17], a nonlinear directional coupler [18], and a nonlinear waveguide junction
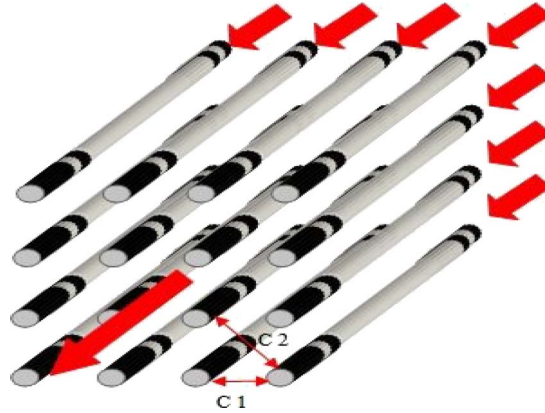
Fig. 1. Two-dimensional array of coupled cavities endowed with a Kerr nonlinearity.

[19]–[21]. Furthermore, a number of experimental and theoretical studies on all-optical logic gates using optical Kerr effect as a switching mechanism have been reported [22]–[25].

The purpose of this work is to introduce 2-D DCSs in Kerr media. This feature of solitons is different compared with its one-dimension counterpart, detailed investigations of which can be found in [8] and [10]. We will show that appropriate Gaussian beam (GB) can be used as a control beam to switch on/off DCSs and to route them, providing an effective tool to use in all-optical logic gates. After introducing the model in Section 2, the bistability of plane wave (PW), DCS is numerically simulated, and their stability is studied in Section 3. In Section 4, the possibility of optical controlling of solitons and its mutual interactions is investigated by demonstrating NOR, XNOR, and NAND logic gates. Finally, Section 5 is devoted to conclusion.

2. Model

We consider a 2-D array of weakly coupled parallel waveguides with Kerr nonlinearity (see Fig. 1). The main assumption is that the evolution of the slowly varying envelopes of the individual guided modes can be described by a discrete equation, taking into account the nearest neighbor interaction of the weakly overlapping guided modes. We assume that the cavities are in resonant with the operating frequency and a mean-field approach can be applied. General discrete model for the normalized amplitude $u_{n,m}$ excited by external driving field E_0 is (Fig. 1):

$$i\frac{\partial u_{n,m}}{\partial t} + C_1(u_{n+1,m} + u_{n-1,m} + u_{n,m+1} + u_{n,m-1} - 4u_{n,m})$$
$$+ C_2(u_{n+1,m+1} + u_{n+1,m-1} + u_{n-1,m+1} + u_{n-1,m-1} - 4u_{n,m})$$
$$+ (\Delta + i)u_{n,m} + \gamma|u_{n,m}|^2 u_{n,m} = E_0 e^{i(q_1 n + q_2 m)}. \tag{1}$$

All quantities are dimensionless, the evolution time, t, is scaled to photon lifetime and the field amplitudes to effective nonlinear coefficient [8], [26]. $u_{n,m}$ is the field amplitude in site (n, m), Δ stands for detuning from the cavity resonance, and C_1 and C_2 are different neighbor coupling between nondiagonal and diagonal cavities, respectively. The evanescent coupling coefficient decreases exponentially with increasing distance between adjacent waveguides. For simplicity, the ratio C_1/C_2 is kept constant to $\sqrt{2}$. The last term at left is self-focusing Kerr nonlinearity in waveguides for $\gamma = +1$. q_1 and q_2 are terms for vertical and horizontal phase shifts between the fields in adjacent cavity inputs that depend on inclination of the holding beam with amplitude E_0.

3. Bistability and Stability Analysis

This system provides two kinds of steady solutions: PW (homogeneous) and localized (DCS) solutions, if $(\partial/\partial t) = 0$.
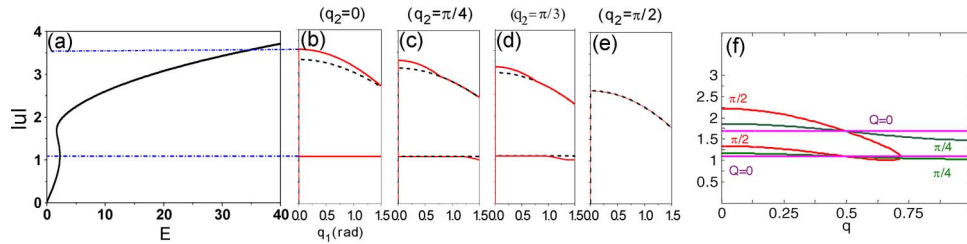
Fig. 2. Bistability curve in terms of PW modulus, $|u|$, versus holding beam amplitude, E_0 (a). Modulationally unstable PW domains in $(|u| - q_1)$-parameter space for various horizontal phase shift, q_2, (b) (c) (d) and (e). MI boundary in the case of considering (neglecting) diagonal waveguide effect is depicted by red-solid (black-dashed) lines. MI for 1-D case is plotted in panel (f) for comparison. (Parameters: $C1 = 0.8$, $C_2 = 0.57$, $\Delta_{eff} = -3$.)

3.1. Homogeneous Solution

Optical bistability and the parametric domain in which system shows two different homogeneous solutions for the same control parameter are essential in existence of solitons. Considering homogeneous solution as $u_{n,m}(t) = u e^{i(q_1 n + q_2 m)}$ gives bistability relation as:

$$E_0 = (1 + \Delta_{eff}^2)|u|^2 + 2\Delta_{eff}\gamma|u|^4 + \gamma^2|u|^6. \qquad (2)$$

This is demonstrated in Fig. 2(a).

The effective detuning is given by:

$$\Delta_{eff} = \Delta + 2C_1(\cos q_1 + \cos q_2 - 2) + 2C_2(\cos(q_1 + q_2) + \cos(q_1 - q_2) - 2).$$

For bistability to be independent of holding beam's phase shift, we consider Δ_{eff} is a constant value (in this case, $\Delta_{eff} = -3$).

Linear stability analysis is used to investigate stability of homogeneous solutions for different parameters and various pump field inclination angles. We study the effects of a small perturbation, with amplitude $a_{n,m}$ and wavenumber Q_1, Q_2.

We suggest the solution as:

$$u_{n,m}(t) = \left[u + a_{n,m} e^{\lambda t + i(Q_1 n + Q_2 m)} \right] e^{i(q_1 n + q_2 m)}. \qquad (3)$$

After some calculation, the eigenvalue λ gives:

$$\lambda = -2iC_1[\sin q_1 \sin Q_1 + \sin q_2 \sin Q_2] - 2iC_2[\cos(Q_1 + q_1)\cos(Q_2 + q_2) - \cos(Q_1 - q_1)\cos(Q_2 - q_2)]$$
$$-1 + \sqrt{\left(\Lambda + \gamma|u|^2\right)\left(\Lambda + 3\gamma|u|^2\right)} \qquad (4)$$

where Λ is:

$$\Lambda = 2C_1[\cos Q_1 \cos q_1 + \cos Q_2 \cos q_2 - 2] + 2C_2[\cos(Q_1 + q_1)\cos(Q_2 + q_2) - 2] + \Delta.$$

This solution becomes unstable if the real part of eigenvalue is positive and vice versa, so to determine the boundary condition for PW stability, we assume $\lambda = 0$. Modulation instability (MI) domains of PW in $-(|u|\_q_1)$-parameter space for different values of q_2 are plotted in Fig. 2(b)–(e) for two different configurations in which the effect of diagonal waveguides is once taken into account and neglected the other time. Fig. 2(f) is to compare stability domain for well-known 1-D case [8].

Fig. 2(a) depicts the modulationally unstable domains of PW in $(|u|\_q_1)$-parameter space for various q_2 values, whereas the dotted lines mark the boundaries of homogenous instability.

It is evident from Fig. 2(b)–(e) the MI domain broadens if one considers the effect of diagonal waveguides. Some initial part of the upper branch is unstable that its top edge is inversely proportional to both q_1 and q_2 values. If the effect of diagonal waveguides is neglected, the lower
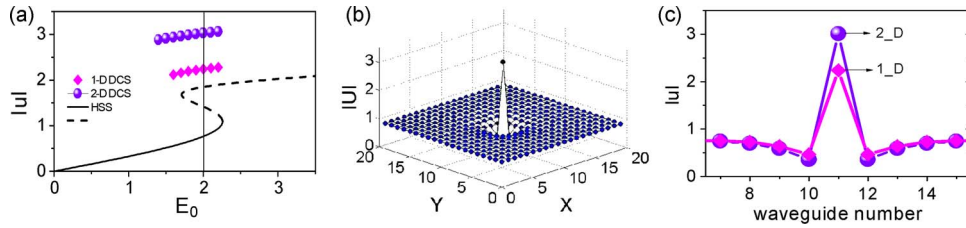
Fig. 3. (a) Families of bright DCSs are shown as maximum modulus of the field amplitude for 1-D (diamond) and for 2-D (circle) with PW solution (solid line: stable and dashed: unstable) versus holding beam amplitude, E_0. (b) Amplitude distribution of 2-D stable DCS. (c) Profiles of DCSs in 1-D (diamond) and 2-D (circle) waveguide array. (Parameters: $E_0 = 2$, $C_1 = 0.8$, $\Delta_{eff} = -3$.)

PW branch is always stable; however, considering diagonal waveguides, sometimes it becomes unstable in parts.

3.2. DCS

The phenomenological theory of DCSs is often based on the discrete NLS equation, and it is valid for weakly coupled waveguides. Here, bright DCSs that propagate along 2-D arrays of cavities endowed with a Kerr nonlinearity are found numerically for a 1-D and a 2-D lattice (see Fig. 3) when holding beam incident normally to the input facet ($q_1 = q_2 = 0$). Newton–Raphson and fourth-order Runge–Kutta methods are used to estimate steady solution of (1) and to investigate time evolution of outgoing beam, respectively. Fig. 3 shows that stable DCS in 2-D not only has larger peak intensity but also exists in a wider range of holding beam with respect to its 1-D counterpart.

4. Controlling of DCSs

The interaction between spatial solitons has attracted much attention because they resemble real particles in the interaction properties. These optical solitons have been concentrated not only for their fundamental interest but also for their potential applications in photonics, optical waveguiding, optical communications, and optical interconnects [27], [28]. In order to optimize the routing/steering process, all-optical control of spatial solitons is highly desirable [25]. In this section, we demonstrate some all-optical controlling of DCS by applying appropriate Gaussian control beam to write, erase and to route. Several all-optical gates are introduced subsequently.

4.1. Switching (Writing and Erasing)

In previous section, existence of bright DCSs and their stability have been investigated. In order to write and erase DCSs in a given site (n, m), we assume holding beam E as a superposition of PW, E_0 and a GB, E_1 as:

$$E = E_0 + E_1 e^{-(n^2+m^2)/w^2} e^{i\phi} \tag{5}$$

where w and ϕ specify width and phase of GB, respectively. Other parameters are fixed as previous section as $E_0 = 2$, $C_1 = 0.8$, $C_2 = 0.57$, and normal incident holding beam is considered, i.e., $q_1 = q_2 = 0$.

The process of writing and erasing of DCS is almost the same, in which GB is injected during t_{inj}, ($\phi = 0$) for writing and out of phase ($\phi = \pi$) for erasing.

The switching process involves two stages: first, injecting of GB, and in the second stage, the system is left to relax to its final stable state. Intensity distributions in adjacent waveguides are shown in Fig. 4. Time evolution of the amplitude during writing and erasing processes and time are plotted in Fig. 5.

Width, intensity, and injection time of applied Gaussian control beam is important in on/off switching. Successful writing and erasing takes place when injection time of GB exceeds a lower threshold depending upon E_1 and w (see Fig. 6). For this purpose, we achieved minimum injection
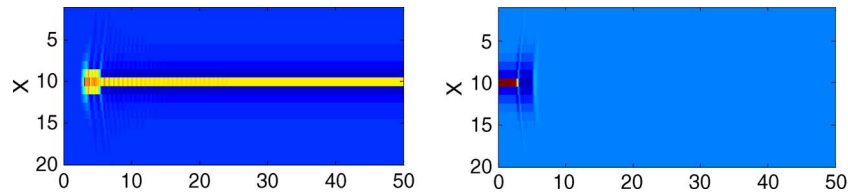
Fig. 4. Panel shows the space–time contour plot of the modulus amplitude of holding beam during writing (left) and erasing (right) processes.
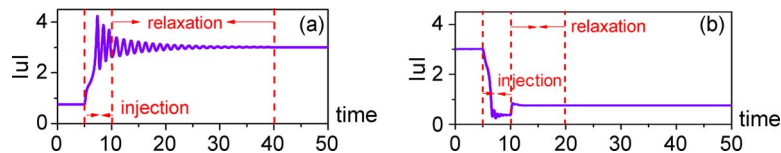
Fig. 5. Time evolutions of peak amplitude during writing and erasing processes in (a) and (b), respectively.
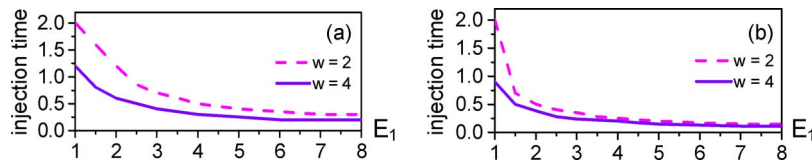
Fig. 6. Injection time versus amplitude of GB E_1 for writing and erasing processes in (a) and (b), respectively, for two different beam widths.

time of control beam for switching (writing and erasing) by increasing control beam amplitude as well as increasing its beam width.

4.2. All-Optical NOR, XNOR, and NAND Gates Based on DCS Interaction

One of the main characteristics of bistable systems is having two distinguished states for the same parameters, which can be considered as logic signal 0 or 1. Furthermore, DCSs in our system that provides locally independent optical information could play a significant role in optical processing issues. So, possibility of designing all-optical logic gates based on DCSs is investigated in this section. Consider two near waveguides named A and B are our input for logic signals. A stable bright soliton in A or B means our signal sets as 1; otherwise, it is 0. For these two near guides to be independent, their distance was chosen to be about 4 waveguides.

The control beam that determines the type of gates is considered as a GB in the form of (5) injected at the waveguide C placed between guides A and B in a short time interval t_{inj}. The gate output is also taken from C after a short time. Interaction of control beam with optical fields in A and B depends on the beam's intensity. Different kinds of gates (NOR, XNOR, and NAND) are designed by well adjusting the intensity of control beam and keeping the injection time fixed at $t_{inj} = 8$, all of which are described in the following subsections in detail.

4.2.1. NOR Gate

The mechanism of a negative-OR (NOR) gate is illustrated in Fig. 6, whereby the information (signals) is guided by two input channels A and B, which are considered to be at $n = 10$ and 14, whereas the device response is controlled at guide C, placed in the middle at $n = 12$, which also used to select gate type. If a GB is injected with $E_1 = 3$, the result would be a NOR gate. In the
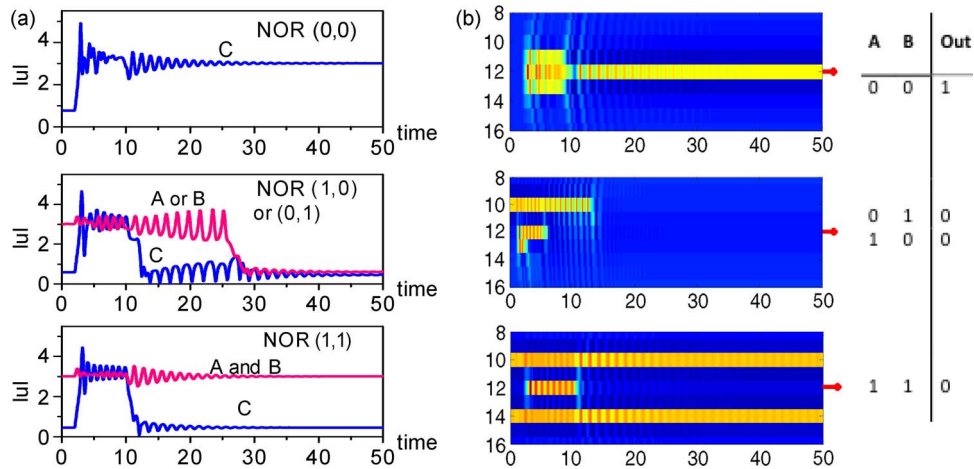
Fig. 7. NOR gate with three soliton-forming beams: A and B are the input signals, and C is the control beam. The table refers to the output. The time evolutions of control and two signal beams (a) and intensity distribution in adjacent waveguides with respect to time for various combinations (b). From top to bottom: both A and B are off (00), only A (or B) on (10), (01) and finally both A and B on (11). The arrow indicates the output channel. Control beam amplitude is $E_1 = 3$, and injection time is $t_{inj} = 8$. Other parameters are $E_0 = 2$, $C1 = 0.8$, $C2 = 0.57$, $\Delta_{eff} = -3$.
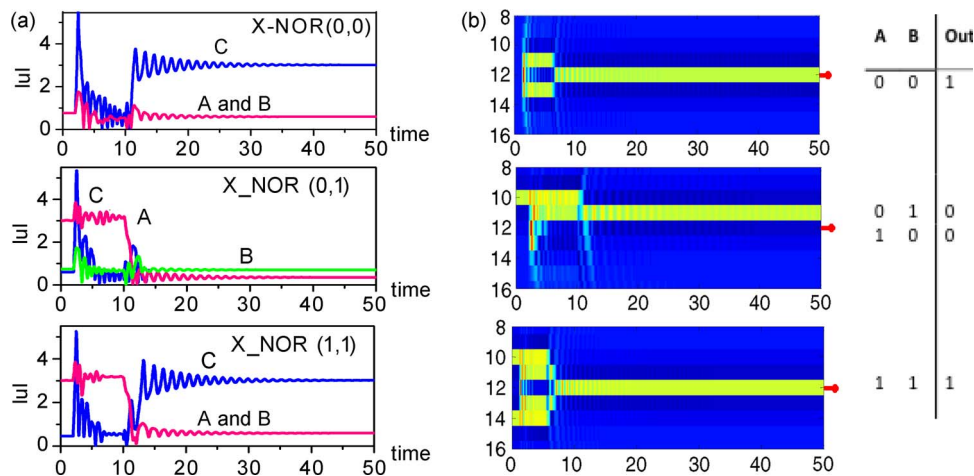
Fig. 8. XNOR gate with three soliton-forming beams. The control and two signal beams time evolutions (a) and intensity distribution in adjacent waveguides with respect to time for various combinations (b). From top to bottom: both A and B are off (00) only A (B) on (10), (01), both A and B on (11). The arrow indicates the output channel. Control beam amplitude is $E_1 = 9$, and injection time is $t_{inj} = 8$. Other parameters are $E_0 = 2$, $C_1 = 0.8$, $C_2 = 0.57$, $\Delta_{eff} = -3$.

absence of any signal in A and B, the injection in C causes a writing process in it, resulting 1 at the end (first row in Fig. 7). However, injection in C has a destructive effect if one of A or B signals is on, resulting 0 (second row). Finally, injection has a transient effect in A and B if both set to 1 and will result 0 (third row). The time evolution of intensity in guides A, B, and C is plotted in Fig. 7(a). Spatial intensity distribution is depicted in Fig. 7(b) for any combination of signals, A and B.

4.2.2. XNOR Gate

Fig. 8 illustrates an exclusive-NOR (XNOR) gate if the injected amplitude of control beam in C is $E_1 = 9$. Control beam can deflect the signal-carrying solitons A or B in each neighbor waveguides, whereas the out port is active only when both or none of A and B are launched.
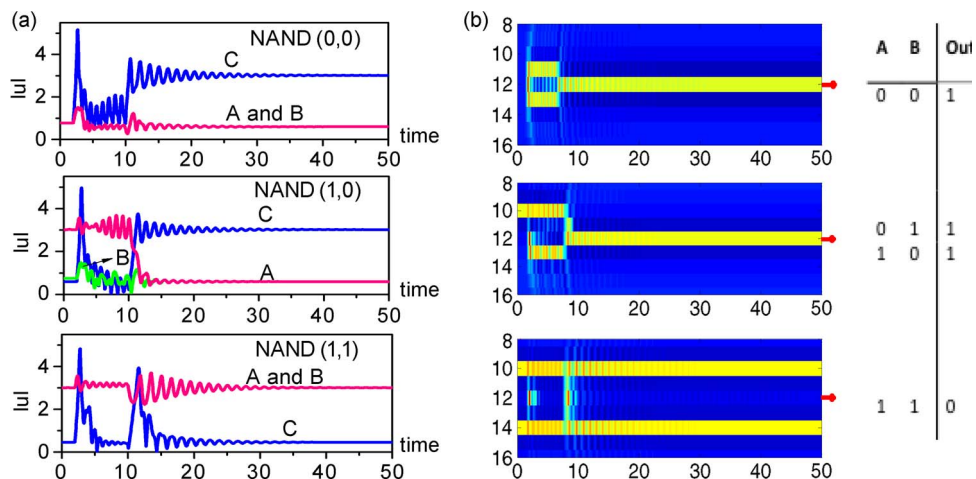
Fig. 9. NAND gate with three soliton-forming beams. The control and two signal beams time evolutions (a) and intensity distribution in adjacent waveguides with respect to time for various combinations (b). From top to bottom: both A and B are off (00) only A (B) on (10), (01), both A and B on (11). The arrow indicates the output channel. Control beam amplitude is $E_1 = 5$, and injection time is $t_{inj} = 8$. Other parameters are $E_0 = 2$, $C1 = 0.8$, $C2 = 0.57$, $\Delta_{eff} = -3$.

4.2.3. NAND Gate

Finally, Fig. 9 is an example of a NAND gate that shows the propagation of A, B, and C, whereas soliton C displays the signal output. As it is apparent from Fig. 9, the output is on when both of the signals are present or absent (with C injected by $E_1 = 5$).

The numerical results show that the proposed all-optical waveguide structure could function as NOR, XNOR, and NAND logic gates by simply setting nonlinear media in selected output guides and properly launching the input power. The all-optical logic gates have potential applications in ultrafast all-optical signal processing and computing systems because of the instantaneous nature of the Kerr nonlinearity, which has no fundamental limits to the achievable speed of operation.

5. Conclusion

In this paper, for the first time to our knowledge, we have investigated 2-D arrays of coupled optical fiber shape cavities. The MI of discrete PWs is analyzed for an arbitrary inclination angle of the holding beam. Existence of single peak spatial soliton is proved numerically in such discrete systems and compared with 1-D case. Successful switch (on/off) of solitons takes place if injection time of writing/erasing beam exceeds a minimum threshold, which is inversely proportional to the amplitude as well as width of the beam. The subsequent section involves the interaction of three propagating beams in 2-D adjacent waveguides. This property is used to demonstrate all-optical logic gates, namely, NOR, XNOR, and NAND. The suggested devices can be used for rapid routing and processing of data in form of optical pulses. This technology also could allow for several further all-optical devices for communication and information processing.

References

[1] F. Lederer, S. Darmanyan, and A. Kobyakov, *Discrete Solitons in Spatial Solitons*, S. Trillo and W. Torruellas, Eds. New York: Springer-Verlag, 2001.
[2] A. Fratalocchi, G. Assanto, and K. A. Brzdakiewicz, "Discrete propagation and spatial solitons in nematic liquid crystals," *Opt. Lett.*, vol. 29, no. 13, pp. 1530–1532, Jul. 2004.
[3] A. Fratalocchi and G. Assanto, "Discrete light localization in one-dimensional nonlinear lattices with arbitrary nonlocality," *Phys. Rev. E, Stat. Phys. Plasmas Fluids Relat. Interdiscip. Top.*, vol. 72, no. 6, p. 066608, Dec. 2005.
[4] U. Peschel, O. A. Egorov, and F. Lederer, "Discrete cavity solitons," *Opt. Lett.*, vol. 29, no. 16, pp. 1909–1911, Aug. 2004.
[5] O. A. Egorov, U. Peschel, and F. Lederer, "Discrete quadratic cavity solitons," *Phys. Rev. E, Stat. Phys. Plasmas Fluids Relat. Interdiscip. Top.*, vol. 71, no. 5, p. 056612, May 2005.

[6] A. V. Yulin, A. R. Champneys, and D. V. Skryabin, "Discrete cavity solitons due to saturable nonlinearity," *Phys. Rev. A, Gen. Phys.*, vol. 78, no. 1, p. 011804R, Jul. 2008.

[7] A. V. Yulin and A. R. Champneys, "Discrete snaking: Multiple cavity solitons in saturable media," *SIAM J. Appl. Dyn. Syst.*, vol. 9, no. 2, pp. 391–431, 2010.

[8] O. A. Egorov, F. Lederer, and Y. S. Kivshar, "How does an inclined holding beam affect discrete modulational instability and solitons in nonlinear cavities?" *Opt. Exp.*, vol. 15, no. 7, pp. 4149–4158, Apr. 2007.

[9] K. M. Aghdami, R. Karimi, and R. Kheradmand, "Control of discrete cavity solitons in coupled cavities," *Phys. Stat. Sol. (C)*, vol. 8, no. 9, pp. 2608–2611, Sep. 2011.

[10] K. M. Aghdami, R. Kheradmand, and R. Karimi, "Switching of multiples solitons in arrays of coupled cavities," *Jpn. J. Appl. Phys.*, vol. 50, no. 5, p. 05FG05, May 2011.

[11] R. A. Vicencio and M. Johansson, "Discrete soliton mobility in two-dimensional waveguide arrays with saturable nonlinearity," *Phys. Rev. E, Stat. Phys. Plasmas Fluids Relat. Interdisc. Top.*, vol. 73, no. 4, p. 046602, 2006.

[12] J. Fleischer, M. Segev, N. Efremidis, and D. Christodoulides, "Observation of two-dimensional discrete solitons in optically induced nonlinear photonic lattices," *Nature*, vol. 422, no. 6928, pp. 147–150, 2003.

[13] D. N. Christodoulides and E. D. Eugenieva, "Blocking and routing discrete solitons in two-dimensional networks of nonlinear waveguide arrays," *Phys. Rev. Lett.*, vol. 87, no. 23, pp. 233901-1–233901-4, 2001.

[14] A. A. Sukhorukov, Y. S. Kivshar, H. S. Eisenberg, and Y. Silberberg, "Spatial optical solitons in waveguide arrays," *Quantum*, vol. 39, no. 1, pp. 31–50, Jan. 2003.

[15] Y. Wu, "New all-optical switch based on the spatial soliton repulsion," *Opt. Exp.*, vol. 14, no. 9, pp. 4005–4012, May 2006.

[16] K. J. Blow, N. J. Doran, and B. K. Nayar, "Experimental demonstration of optical soliton switching in an all-fiber nonlinear Sagnac interferometer," *Opt. Lett.*, vol. 14, no. 14, pp. 754–756, Jul. 1989.

[17] L. Thylen, N. Finalayson, C. T. Seaton, and G. I. Stegeman, "All-optical guided-wave Mach–Zehnder switching device," *Appl. Phys. Lett.*, vol. 51, pp. 1304–1306, Oct. 1987.

[18] S. R. Friberg, A. M. Weiner, Y. Silberberg, B. G. Sfez, and P. S. Smith, "Femtosecond switching in dual-core-fiber nonlinear coupler," *Opt. Lett.*, vol. 13, no. 10, pp. 904–906, Oct. 1988.

[19] Y. Silberberg and B. G. Sfez, "All-optical phase- and power-controlled switching in nonlinear waveguide junctions," *Opt. Lett.*, vol. 13, no. 12, pp. 1132–1134, Dec. 1988.

[20] J. P. Sabini, N. Finalyson, and G. I. Stegeman, "All-optical switching in nonlinear X junctions," *Appl. Phys. Lett.*, vol. 55, no. 12, pp. 1176–1178, Sep. 1989.

[21] H. Fouckhardt and Y. Silberberg, "All-optical switching in waveguide X junctions," *J. Opt. Soc. Amer. B, Opt. Phys.*, vol. 7, no. 5, pp. 803–809, May 1990.

[22] T. Yabu, M. Geshiro, T. Kitamura, K. Nishida, and S. Sawa, "All-optical logic gates containing a two-mode nonlinear waveguides," *IEEE J. Quantum Electron.*, vol. 38, no. 1, pp. 37–46, Jan. 2002.

[23] Y. D. Wu, "All-optical logic gates by using multibranch waveguide structure with localized optical nonlinearity," *IEEE J. Sel. Topics Quantum Electron.*, vol. 11, no. 2, pp. 307–312, Mar./Apr. 2005.

[24] M. Peccianti, C. Conti, G. Assanto, A. De Luca, and C. Umeton, "All optical switching and logic gating with spatial solitons in liquid crystals," *Appl. Phys. Lett.*, vol. 81, no. 18, pp. 3335–3337, Oct. 2002.

[25] A. Piccardi, A. Alberucci, G. Assanto, U. Bortolozzo, and S. Residori, "Soliton gating and switching in liquid crystal light valve," *Appl. Phys. Lett.*, vol. 96, no. 7, pp. 071104-1–071104-3, Feb. 2010.

[26] B. Feng and T. Kawahara, *Discrete Breathers in Two-Dimensional Nonlinear Lattices.*   Amsterdam, The Netherlands: Elsevier, 2007, ISSN: 0165-2125.

[27] F. Lederer, G. I. Stegeman, D. N. Christodoulides, G. Assanto, M. Segev, and Y. Silberberg, "Discrete solitons in optics," *Phys. Rep.*, vol. 463, no. 1–3, pp. 1–126, 2008.

[28] M. Peccianti and G. Assanto, "Signal readdressing by steering of spatial solitons in bulk nematic liquid crystals," *Opt. Lett.*, vol. 26, no. 21, pp. 1690–1692, Nov. 2001.